Chapter 12

Integrating Well Test–Derived Effective Absolute Permeabilities in Geostatistical Reservoir Modeling

Clayton V. Deutsch
Exxon Production Research Company
Houston, Texas, U.S.A.

André G. Journel
Department of Petroleum Engineering
Stanford University
Stanford, California, U.S.A.

ABSTRACT

In many cases, an estimate of effective absolute permeability may be derived from a pressure-transient well test. This effective permeability does not resolve local details of the permeability distribution; however, it does constrain the average permeability in the vicinity of the well. This paper presents an approach, based on simulated annealing, that integrates well test–derived effective permeabilities in stochastic reservoir models.

The volume and type of averaging informed by the well test must first be calibrated by forward simulating the well test on stochastic reservoir models that are consistent with the geological interpretation, core, well log, and seismic data. Stochastic reservoir models are then constructed with simulated annealing to additionally honor the well test–derived average permeabilities.

We present an example that illustrates how the methodology is implemented in practice. The improvement in the stochastic reservoir models is demonstrated by more accurate and precise prediction of future reservoir performance.

INTRODUCTION

The concept underlying stochastic reservoir modeling is to construct numerical models of the reservoir properties that are consistent with all relevant data. History matching is easier and forward predictions are more reliable when the numerical geological models honor more information. Applying a flow simulator to multiple numerical models allows an appreciation for the uncertainty in the reservoir response. A maximum amount of relevant prior information, e.g., core measurements, log data, geophysical data, geological inter-

pretations, and well test data, must be integrated to ensure realistic output from the simulator. This chapter is concerned with integrating effective permeabilities derived from pressure-transient well tests into stochastic models of absolute permeability.

Conventional conditional simulation techniques such as Gaussian (Matheron et al., 1987; Deutsch and Journel, 1992), fractal (Hewett, 1986), or indicator (Journel and Alabert, 1990) models have the ability to account for local conditioning data (core and well log data), a global histogram, and varying amounts of spatial information in the form of variogram models. Variants of these techniques based on cokriging (Doyen et al., 1988) or some type of trend model (Marechal, 1984) allow geophysical information to be integrated into the resulting realizations. None of these techniques, however, allow the integration of well test–derived effective permeabilities.

Simulation techniques based on marked point processes (Haldorsen and Damsleth, 1990) are well suited to simulating spatial phenomena characterized by a repetition of easily depicted shapes. The resulting spatial structure is implicitly controlled by the placement of the digitized or analytically defined objects. Conditioning to local data and a global histogram is achieved by disallowing inconsistencies at data locations and controlling the number of objects placed in the realization. The integration of geophysical interpretations and well test–derived effective permeabilities is difficult with these latter techniques.

A well test–derived effective permeability does not directly resolve the smaller scale permeability values near the well bore; however, it does account for a complex nonlinear average of the small-scale values. Flow simulation results are directly influenced by the average flow characteristics as indicated by well test–derived effective permeabilities. Historically, well test–derived permeabilities were used in homogeneous reservoir models for reservoir performance forecasting (Ramey, 1990). Two inadequacies of such homogeneous and deterministic models are that they do not allow one to assess uncertainty and they do not allow for the important influence of small-scale permeability heterogeneities. Stochastic reservoir models allow the small-scale permeability heterogeneities to be accounted for; however, as mentioned, current stochastic modeling techniques do not account for the information carried by average properties measured by well tests.

Another possible method to account for well test–derived permeabilities is to rescale the core or well log–derived permeability values such that the permeability/thickness product of the core data is the same as the well test result. This method may be appropriate when the well test is measuring a different component of the permeability, such as fractures. We do not address this issue in this chapter. The assumption made here is that the core and well log data are representative and their spatial distribution may be altered to reproduce the well test result.

The problem of conditioning stochastic models to well test–derived effective permeability is difficult because the average is nonlinear. Conventional simulation techniques allow data of different volumetric supports only when the averaging is linear (Journel and Huijbregts, 1978).

One way to achieve this conditioning would be to discard all models that do not yield a forward-simulated well test response close enough to the actual measured pressure response. Such selection procedures may be practical when building models with a single well test; it is not practical, however, in the presence of multiple well test interpretations, some based on more advanced multirate tests, that give a number of different permeability averages near the well. In general, a prohibitively large number of realizations would be required to find a few that simultaneously match all well test data.

The algorithm proposed in this paper generates realizations with simulated annealing (Kirkpatrick et al., 1983) that honor the measured well test effective permeabilities in addition to conventional data, such as the local log-derived permeability values data, a histogram, and a variogram. The application of simulated annealing requires that the generation of a stochastic realization be posed as an optimization problem. The two-part objective function in this optimization problem consists of the deviation from the model variogram plus the deviation from the well test effective permeabilities. The deviation from the measured well test results could be known through forward simulation of the well test on all candidate realizations. Again, it would be impractical to forward simulate the well test after each perturbation as demanded by simulated annealing; therefore, the forward simulation must be replaced by a more easily calculated numerical approximation. A nonlinear power average (Korvin, 1981; Deutsch, 1987; Alabert, 1989) of the small-scale permeability values has been adopted for this purpose.

More precisely, the well test is first interpreted to provide the effective permeability-thickness product near the well bore. The effective permeability is computed knowing the reservoir thickness. Then, the type of averaging, as quantified by an averaging power, and the volume of averaging must be calibrated. The averaging power depends essentially on the connectivity of the extreme permeability values. The volume of averaging depends on the duration of the well test. Finally, the initial stochastic realizations are altered by systematically changing the elementary grid block permeability values so that the previously calculated effective permeability and the variogram model are honored. The effective permeability can be calculated very fast after each perturbation using the previously calibrated power average.

The following algorithm will clarify the implementation details and acknowledge a number of limitations. One limitation is that the method imposes the well test results without accounting for uncertainty in the underlying well test interpretation. A second limitation is that the method requires that the full well test response be summarized by a single nonlinear weighted power average. The

severity of these limitations may be judged through numerical experimentation.

QUANTIFYING WELL TEST–DERIVED EFFECTIVE PERMEABILITY

Pressure transient well tests are performed by generating a flow rate impulse in the reservoir and measuring the pressure response. Well test interpretation consists of interpreting the pressure response by using an appropriate mathematical model to relate the pressure response (output) to flow rate history (input) (Horne, 1990). Provided that the mathematical model is appropriate, the model parameters can be associated to certain reservoir parameters. Of particular interest is the effective absolute permeability k_e.

To apply the envisaged optimization technique it is necessary to translate this well test–derived k_e into a more easily calculated property while retaining the flexibility to differentiate a wide variety of heterogeneous systems encountered in practice. The power averaging formalism is used to model the nonlinear averaging of absolute permeabilities (equation 1). The assumption is that the elementary permeability values average linearly after a nonlinear power transformation, that is

$$\bar{k}(\omega) = \left[\frac{1}{N} \sum_{u_i \in V} k(u_i)^{\omega} \right]^{\frac{1}{\omega}} \tag{1}$$

where $\bar{k}(\omega)$ is the ω-power average permeability of the N permeability values $k(u_i)$, $i = 1,\ldots,N$, at locations u_i within the volume of interest V. The power ω ranges between the bounding values of –1 and 1 corresponding to the harmonic and arithmetic averages, respectively (the geometric average is obtained for $\omega = 0.0$). The idea is to use relation (1) and to calibrate the averaging volume V and averaging power ω for each particular well test.

To define the appropriate averaging volume it is necessary to consider the portion of the pressure response used to derive the well test effective permeability k_e. In practice, k_e is obtained by interpreting the pressure response during the time at which the response resembles infinite-acting radial flow. Early time effects, such as well-bore storage, and late time boundary effects are not considered in the interpretation. It is possible to define an inner radius r_{min} and an outer radius r_{max} that correspond to the time limits of the interpretation because the pressure response, at any time t, may be related to block permeabilities within a time-dependent radius of drainage $r(t)$. Consider a typical pressure response shown on the Miller-Dyes-Hutchinson (MDH) plot in Figure 1. The pressure response between 1 and 10 hr is used to derive an estimate of the effective permeability $k_{welltest}$. The inner and outer limits of the shaded region (on the schematic illustration of the reservoir) correspond to the radius of drainage at 1 and 10 hr, respectively. Actually, these limits will not be circular due to local heterogeneities. The impact of this assumption will be revealed in the experimental calibration described in a following section.

The time interval during which the pressure response resembles infinite-acting radial flow is easily determined by standard interpretation techniques. Evaluating the radius of drainage $r(t)$ at the time limits is not as straightforward; depending on the arbitrary definition chosen for $r(t)$, the radius can change by as much as a factor of 4. It will be necessary to calibrate the radius of drainage $r(t)$ by repeated flow simulations. The block permeabilities contributing to the pressure response measured up to time t are approximately enclosed by a circular volume centered at the well and defined by a time-dependent radius $r(t)$ written as (van Poollen, 1964; Johnson, 1988; Alabert, 1989)

$$r(t) = A\sqrt{\frac{k_e t}{\phi \mu c_t}} \tag{2}$$

where A is a constant, k_e is the reservoir permeability around the well, ϕ is the porosity, μ is the fluid viscosity, and c_t is the total compressibility. Depending on the definition chosen for the radius of drainage, the value of A ranges from 0.023 to 0.07 (for oil field units). Alabert (1989), in evaluating the averaging volume of a well test and for specified levels of discretization and test durations, found an optimal A_{opt} value of 0.010 in oil field units.

The averaging power ω describes the type of averaging within the volume. In many cases, this averaging power is close to the geometric average ($\omega = 0$). For

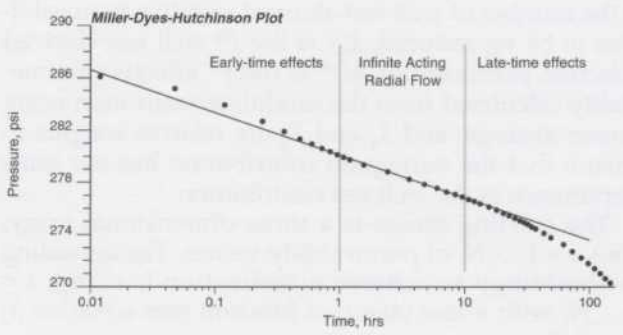

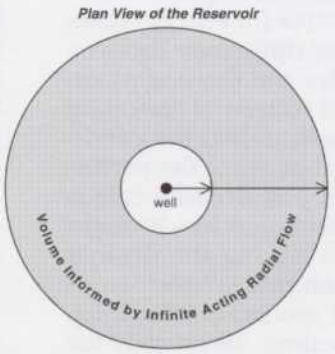

Figure 1. A schematic illustration of the volume measured by a given well test interpretation. The inner and outer limits of the shaded region, on the plan view of the reservoir, correspond to the radius-of-drainage at 1 and 10 hr, respectively (the limits of infinite acting radial flow).

practical test durations and for complex heterogeneous permeability distributions, the type of averaging can differ significantly from the geometric average.

There are no reliable universal values for the constant A and the averaging power ω; they must be calibrated using the following procedure (see also Alabert, 1989; Deutsch, 1992).

1. Generate n_s (20–100) multiple realizations of the permeability field with relevant statistical properties.
2. Forward simulate a well test, with conditions as close as possible to those used in the field to arrive at k_e, on each realization to obtain n_s pressure response curves.
3. Deduce an effective permeability $\bar{k}_i$, $i = 1,\ldots,n_s$ from each pressure curve using established well test interpretation techniques (Horne, 1990).
4. Compute average permeabilities $\bar{k}(A,\omega)_i$, $i = 1,\ldots,n_s$ for A values between the practical bounding limits of 0.001 and 0.020 and for ω values between practical bounding limits of –0.5 and 0.5.
5. Choose the pair (A_{opt},ω_{opt}) that yields the closest agreement between the reference $\bar{k}_i$, $i = 1, \ldots, n_s$ values and the approximate $\bar{k}(A_{opt},\omega_{opt})_i$, $i = 1,\ldots,n_s$ values.

After establishing appropriate A_{opt} and ω_{opt} values the validity of the power average approximation can be checked by creating a scatterplot of the $\bar{k}\,(A_{opt},\omega_{opt})_i$ values versus the well test–derived $\bar{k}_i$ values.

In summary, the weighted nonlinear power average (equation 1) is proposed as a computationally simple replacement for the full well test response. In practice, a well test response is interpreted to yield an estimate of the effective permeability k_e and the averaging volume parameter A_{opt} and power ω_{opt} are calibrated for the particular geological setting. The next step is to impose the well test–derived effective permeability k_e, i.e., the appropriate ω average $\bar{k}\,(A_{opt},\omega_{opt})$, on stochastic models. We use the technique of simulated annealing.

SIMULATED ANNEALING

The "annealing" approach to stochastic simulation has no explicit random function model, rather the creation of a simulated realization is formulated as an optimization problem. The first requirement of this class of methods is an objective (or energy) function, which is some measure of difference between the desired spatial characteristics and those of a candidate realization. The essential feature of annealing methods is to iteratively perturb (relax) the candidate realization and then accept or reject the perturbation with some decision rule. The decision rule is based on how much the perturbation has brought the candidate image closer to having the desired properties. One possible decision rule is based on an analogy with the metallurgical process of annealing, hence the name simulated annealing. Technically the name "simulated annealing" applies only to those stochastic relaxation methods based strictly on simulated annealing (Aarts and Korts, 1989; Kirkpatrick et al., 1983); however, through common usage the name "annealing" is used to describe the entire family of methods that are based on the principle of stochastic relaxation.

Annealing is the process where a metallic alloy is heated so that molecules may move positions relative to one another and reorder themselves into a low-energy crystal (or grain) structure. The probability that any two molecules will move relative to one another is known to follow the Boltzmann probability distribution. Simulated annealing is the application of the annealing mechanism of perturbation (swap the attribute values assigned to two different grid node locations) with the Boltzmann probability distribution for accepting perturbations.

At first glance this approach appears terribly inefficient. For example, millions of perturbations may be required to arrive at an image that has the desired spatial structure. However, these methods are more efficient than they might seem as long as few arithmetic operations are used to update the objective function after a perturbation; virtually all conventional global spatial statistics (e.g., a variogram) may be updated locally rather than globally recalculated after a local perturbation. Also, the power average representation of the well test k_e developed earlier is easily updated.

The objective function is defined as some measure of difference between a set of reference properties and the corresponding properties of a candidate realization. The reference properties could consist of any quantified geological, statistical, or engineering property. In the context of this paper, the reference properties consist of traditional variogram functions and the well test–derived effective permeability. Thus, the objective function could be written as

$$O = \lambda_1 \times \sum_{i=1}^{n_h} \left[\gamma^{ref}(\mathbf{h}_i) - \gamma^{real}(\mathbf{h}_i)\right]^2 + \lambda_2 \times \sum_{j=1}^{n_K} \left[k_{e_j}^{ref} - k_{e_j}^{real}\right]^2 \quad (3)$$

where O is the objective function, n_h is the number of variogram lags, $\boldsymbol{h}_i$ considered important, $\gamma^{ref}(\boldsymbol{h}_i)$ is the reference variogram value for lag $\boldsymbol{h}_i$, $\gamma^{real}(\boldsymbol{h}_i)$ is the variogram value taken from the candidate realization, n_K is the number of well test–derived effective permeabilities to be reproduced, $k_{e_j}^{ref}$ is the j^{th} well test–derived effective permeability, $k_{e_j}^{real}$ is the j^{th} effective permeability calculated from the candidate realization using power average, and λ_1 and λ_2 are relative weights to ensure that the variogram contribution has the same importance as the well test contribution.

The starting image is a three-dimensional array, $z(\boldsymbol{u}_i)$, $i = 1,\ldots,N$, of permeability values. The annealing methodology to achieve a realization l, $z^{(l)}(\boldsymbol{u}_i)$, $i = 1,\ldots,N$, with a low objective function (see equation 3) is as follows.

1. Generate an easily constructed initial realization: the initial realization is either the output of a more conventional stochastic simulation algorithm or the initial realization could be generated by assigning each nodal value at random from the stationary univariate distribution $F(z)$.
2. Establish the reference components in the objective function: the reference variogram values $\gamma^{ref}(\boldsymbol{h}_i)$, $i = 1,\ldots,n_h$ are based on experimental data or on an analytical model. The reference effective permeabilities k_{ej}^{ref} $j = 1,\ldots,n_K$, are the direct result of applying standard interpretation techniques to the pressure transient responses measured in the field.
3. Compute the realization components in the objective function: the variogram values $\gamma^{real}(\boldsymbol{h}_i)$, $i = 1,\ldots,n_h$, and the effective permeabilities k_{ej}^{real} $j = 1,\ldots,n_K$, are calculated from the candidate realization.
4. Compute the objective function O based on the reference and the realization statistics (see equation 3).
5. Perturb the realization to generate a new realization by swapping the permeability values at any two locations.
6. Update each component in the objective function and recompute the objective function O_{new} with the perturbation. The change to the objective function is $\Delta O = O_{new} - O_{old}$.
7. The perturbation is accepted or rejected on the basis of a specified decision rule. One approach would be to accept all helpful perturbations $\Delta O \leq 0.0$ and to reject all disruptive perturbations $\Delta O > 0.0$. This choice, which corresponds to a steepest descent approach, can lead to a local minimum. The essential contribution of simulated annealing is a prescription for when to accept or reject a given perturbation. The acceptance probability distribution is given by

$$P\{accept\} = \begin{cases} 1, & \text{if } \Delta O \leq 0.0 \\ \dfrac{-\Delta O}{e^{t}}, & \text{otherwise} \end{cases} \tag{4}$$

   All favorable perturbations ($\Delta O \leq 0.0$) are accepted and some unfavorable perturbations are accepted with an exponential probability distribution. The parameter t of the exponential distribution is analogous to the "temperature" in annealing. The higher the temperature, the more likely an unfavorable perturbation will be accepted. Accepting the perturbation causes the image $z(\boldsymbol{u}_i)$, $i = 1,\ldots,N$ and the objective function O to be updated.
8. When the objective function O gets close to zero then the realization is considered finished because it now honors both the reference variogram and the well test data; otherwise, return to step 5 and continue the perturbation process.

The idea is to start with an initially high temperature parameter t and lower it by some multiplicative factor λ (say 0.1) when enough perturbations have been accepted (K_{accept} = 10 times the number N of grid nodes in the system) or too many have been tried ($K_{max} = 100 \times N$). The algorithm is stopped when efforts to lower the objective function become sufficiently discouraging (Press et al., 1986).

One remaining issue is to establish the weights λ_1 and λ_2 applied to each component in the objective function. The purpose behind these weights is to have each component play an equally important role in the global objective function. Without any weighting, the component with the largest units would dominate the objective function. The weights λ_1 and λ_2 are established so that, on average, each component contributes equally to a change in the objective function ΔO. That is, each weight λ_c is inversely proportional to the average change of that component objective function:

$$\lambda_c = \frac{1}{\overline{|\Delta O_c|}}, \quad c = 1,\ldots,2 \tag{5}$$

In practice, the average change of each component $\overline{|\Delta O_c|}$ cannot be computed analytically; however, it can be numerically approximated by evaluating the average change of M (say 1000) independent perturbations:

$$\overline{|\Delta O_c|} = \frac{1}{M}\sum_{m=1}^{M}\left|O_c^{(m)} - O_c\right|, \quad c = 1,\ldots,2 \tag{6}$$

where $\overline{|\Delta O_c|}$ is the average change for component c, $O_c^{(m)}$ is the perturbed objective value, and O_c is the initial objective value. Each of the M perturbations $m = 1,\ldots,M$ arises from the swapping mechanism employed for the annealing simulation.

All of the elements needed for integrating well test data are now in place. The resulting realizations obtained after going through the simulated annealing procedure with the objective function (see equation 3) are conditional to both the initial geological/statistical description and the well test–derived permeabilities. The following example illustrates how the methodology is implemented in practice.

AN EXAMPLE APPLICATION

Consider an example where the block horizontal absolute permeabilities are known to follow a distribution $F(z)$, which results from the sum of a constant 2.5 md and a lognormal component with a mean of 10.0 md and a variance of 225 md^2. This two-part distribution reflects the simplifying assumption of representing a three-dimensional permeability distribution by a two-dimensional areal model. The two-dimensional spatial distribution of permeability is characterized by a spherical normal scores variogram model $\gamma_Y(\boldsymbol{h})$ with a range of 25 grid block units. A 101 × 101 unit realization of this lognormal permeability field was generated to serve as a reference distribution (Figure 2). A core (or well log–derived) permeability and a drawdown well test–derived permeability are known at the five

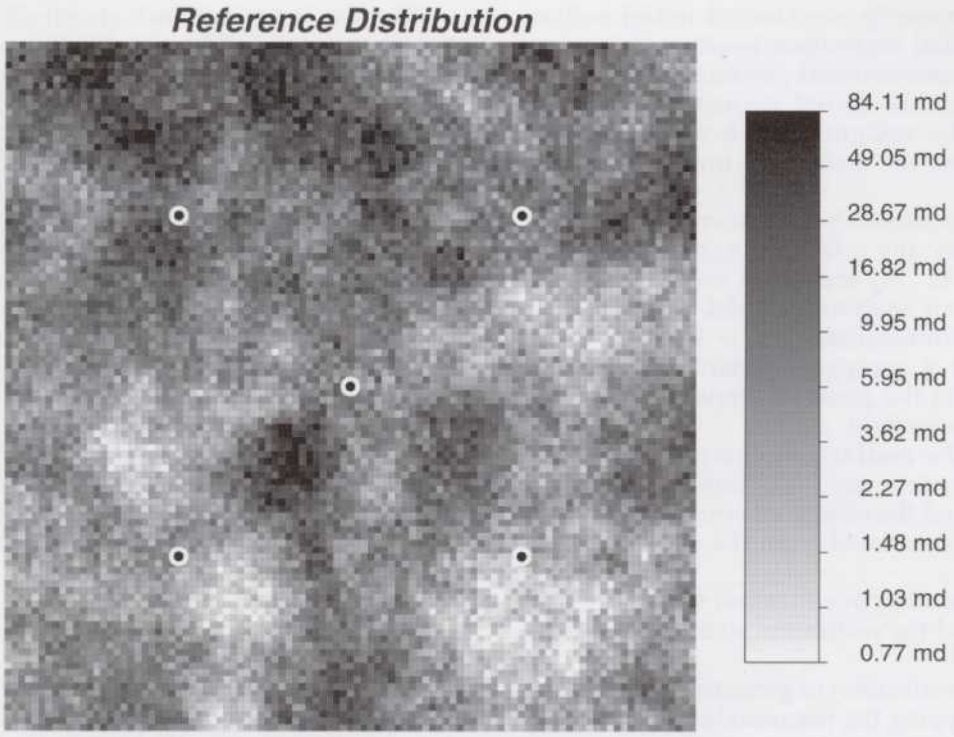

Figure 2. The reference distribution of permeability considered as the true reservoir for the purposes of obtaining the well test responses and interpreted effective permeabilities. The conditioning data, falling on a five-spot pattern, are highlighted by the black dots.

well locations (see Table 1). The five drawdown pressure response curves are shown on Figure 3.

Simulated annealing was used to generate 100 realizations conditional to the distribution model $F(z)$, the variogram model $\gamma_Y(\boldsymbol{h})$, and the five core data; the following objective function was considered:

$$O = \sum_{i=1}^{n_h} \left[\gamma^{ref}(\mathbf{h}_i) - \gamma^{real}(\mathbf{h}_i)\right]^2$$

where n_h corresponds to the most compact arrangement of 200 lags (Figure 4). Annealing allows this objective function to be reduced close to zero, i.e., the resulting realizations provide an excellent reproduction of the variogram. The first four realizations are shown on Figure 5.

These 100 initial realizations reproduce the core permeability at the five well locations. The well test values, however, are not reproduced. Figure 6 shows five histograms of the well test–derived permeability values obtained from the 100 simulated realizations. The vertical line in each histogram is the result of the reference case. Ideally, the realizations would be conditional to the reference well test values.

To check the validity of the numerical well test simulation, the five well tests were simulated using uniform permeability fields. The results for all five wells with three different uniform permeability fields (5.0, 10.0, and 50.0 md) are shown on Figure 7. The time limits for infinite acting radial flow are shown by the vertical lines. The well test–derived effective permeabilities are shown on Table 2. The well test–derived values appear consistently lower than the input permeability field; all of the wells show the same bias. This bias was not considered significant for permeabilities of less than 50 md. Additional validation runs would be warranted if well test–derived permeability values were observed outside of this range.

These 100 effective permeability values, derived from forward simulating the well test on 100 unconditional realizations, were used to calibrate the parame-

Table 1. Core- and well test–derived effective absolute permeability from five wells in the study area

Well	Core Permeability (md)	Well Test Permeability (md)
1 (top left*)	7.25	14.16
2 (top right)	10.95	9.63
3 (center)	8.89	9.41
4 (bottom left)	5.04	5.59
5 (bottom right)	4.03	4.54

*Position in parentheses refers to well positions shown in Figure 2.

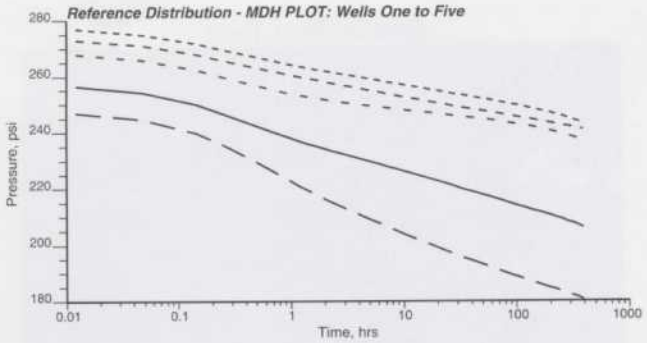

Figure 3. The pressure response for the five wells is shown on this Miller-Dyes-Hutchinson (MDH) plot.

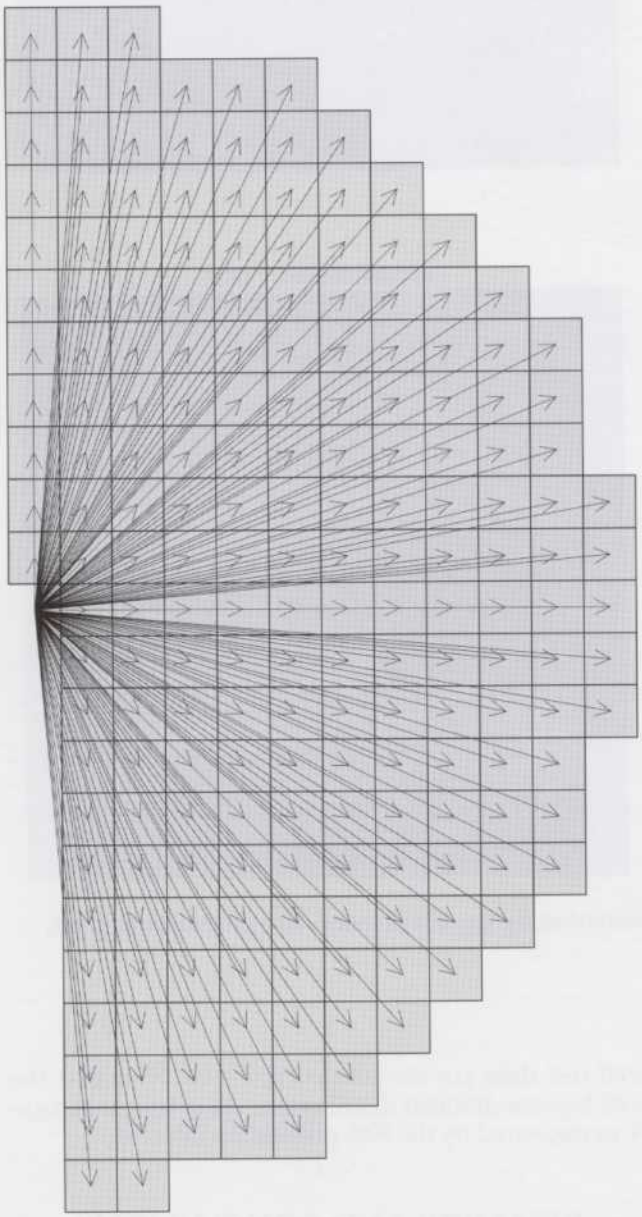

Figure 4. A polar plot of the 200 lag vectors that enter the objective function of the annealing simulation.

Table 2. Well test–derived effective absolute permeabilities from uniform permeability fields*

	Uniform Permeability Fields (md)		
Well	**5.00**	**10.00**	**50.00**
1 (top left**)	4.96	9.99	48.75
2 (top right)	4.96	9.99	48.77
3 (center)	4.96	10.00	48.80
4 (bottom left)	4.96	9.98	48.73
5 (bottom right)	4.96	9.99	48.75
Difference (%)	–0.1	–0.1	–2.5

*Simulated values appear slightly lower than those of the uniform permeability field.
**Position in parentheses refers to well positions shown in Figure 2.

ters A_{opt} and ω_{opt} that provide the best numerical approximation to the well test result. The average permeabilities $k\,(A,\omega)_i$, $i = 1,\ldots,n_s$ for A values between the practical bounding limits of 0.001 and 0.020 and for ω values between practical bounding limits of –0.5 and 0.5 were computed using the 100 initial realizations. The criteria for an optimal pair (A_{opt},ω_{opt}) was to simultaneously maximize the correlation and minimize the bias between the power average approximation (equation 1) and the true well test values. The optimal pair A_{opt} = 0.003 and ω_{opt} = 0.0 was found to both maximize the correlation and minimize the bias.

Figure 8 shows a scatterplot of the power average numerical approximation and the true well test–derived effective permeability. Note the lack of any bias (the average effective permeabilities are 9.3 md in both cases) and the excellent correlation of 0.83. The physical volume informed by the well test can be determined by the constant A_{opt} and knowledge of the time limits of the infinite acting portion of the pressure response: r_{min} = 1.0 grid units (70.1 ft) and r_{max} = 4.6 grid units (320.0 ft).

The annealing simulation now uses a two-part objective function (equation 3). Annealing is able to generate realizations that lower this objective function to zero. The first four realizations are shown on Figure 9.

To verify that the calibrated power average is a fair approximation of the actual well test result, a full well test was forward simulated on the final 100 realizations. The distributions of effective permeabilities, after processing, is extremely close to the reference values.

This illustrates that well test effective permeabilities can be imposed on stochastic realizations to a fair degree of approximation. What has not been shown yet is that accounting for well test–derived effective permeability actually helps predict future reservoir performance. To illustrate the improvement in future prediction, all 201 realizations (the reference, the 100 initial, and the 100 well test–conditioned realizations) have been associated to the five-spot injection/production pattern shown on Figure 2 with an injector at all corner locations and a central producer. All variables except the block absolute permeabilities have been held constant and the performance of each realization

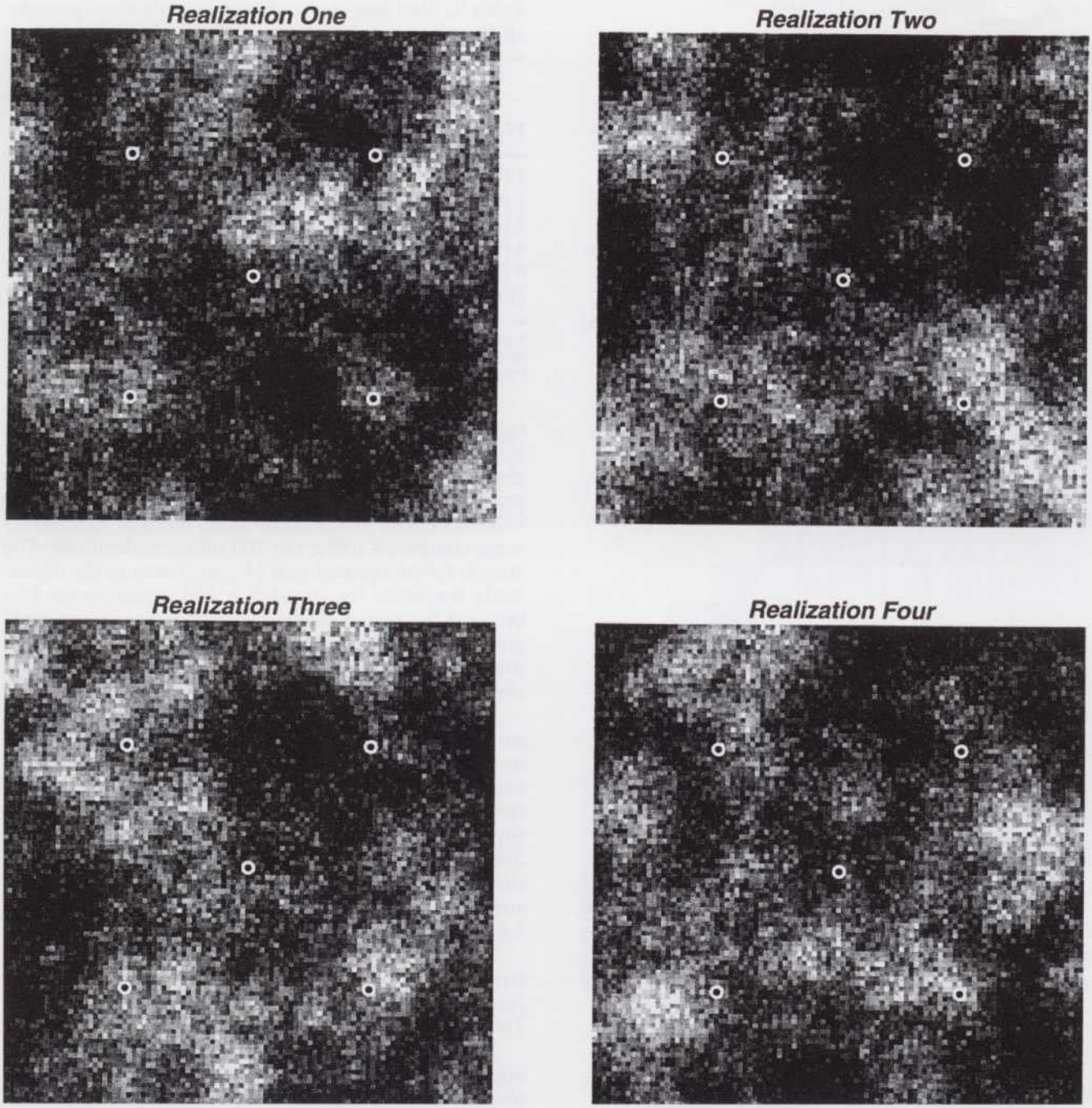

Figure 5. Four realizations conditional to the five data (represented by the black dots), the global histogram, and the global variogram.

has been simulated with ECLIPSE (Exploration Consultants Limited, 1984).

Three response variables are presented here: (1) the time to reach 90% water cut, (2) the time of first water arrival at the producer, and (3) the time to reach 50% water cut (the units are important only in a relative sense). The reference image yielded response variables of 86.8, 8.93, and 20.8, respectively. The histograms of values obtained before and after conditioning to the well test data are shown on Figure 10. Note that the well test–conditioned distributions show less uncertainty as measured by the 90% probability interval.

REMARKS AND CONCLUSIONS

Our methodology integrates well test–derived properties into stochastic reservoir models. The

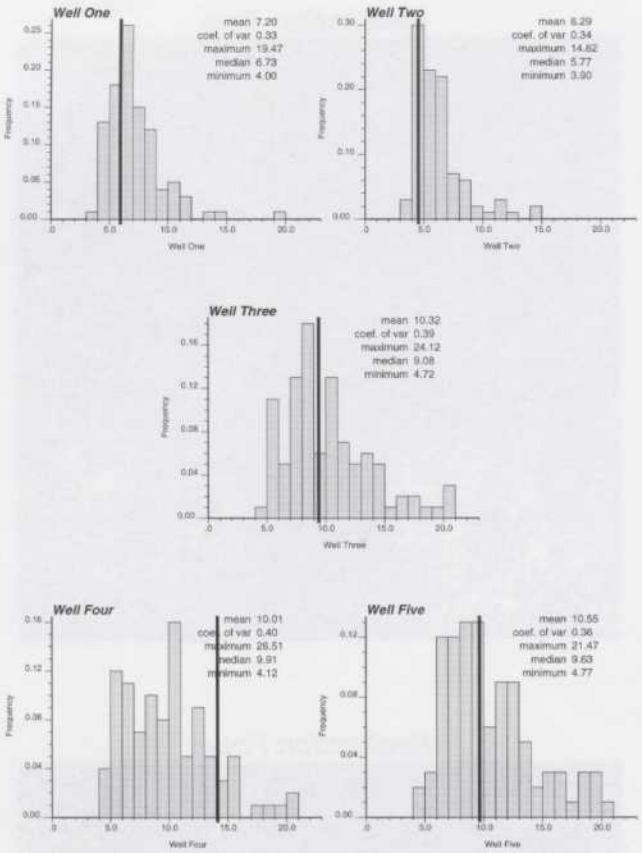

Figure 6. The well test–derived effective absolute permeabilities for each of the five wells. One hundred realizations were generated and five well test simulations were performed on each realization to obtain these histograms.

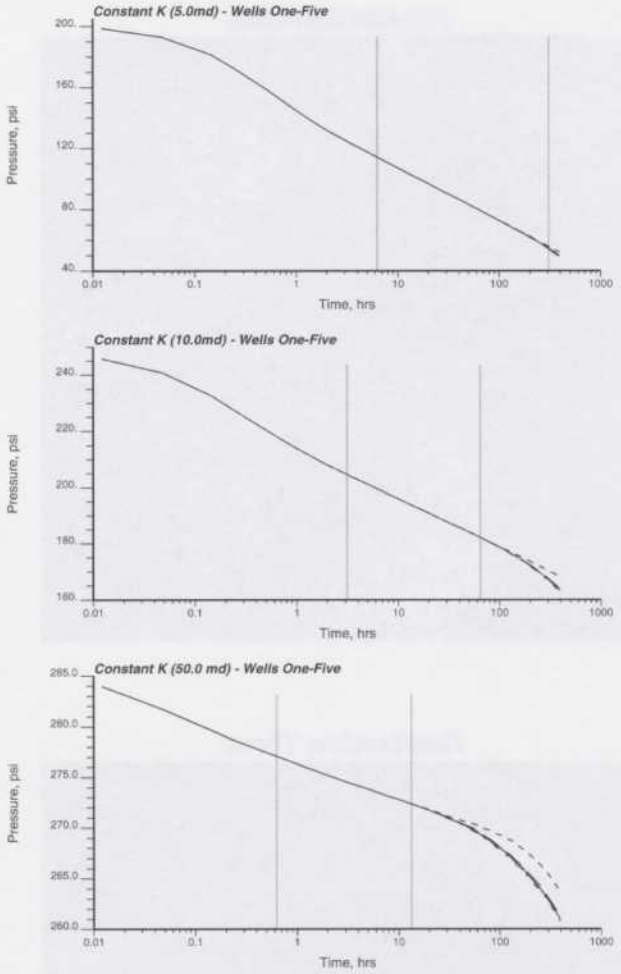

Figure 7. The well test response for three different uniform permeability cases. The response and interpreted results are shown for all five wells in the five-spot pattern.

methodology consists of generating realizations with simulated annealing. The objective is to minimize deviations from the initial variogram model and yet honor a numerical approximation of the well test–derived effective permeability. The power average numerical approximation is useful because it would not be feasible to rerun a flow simulation after each perturbation called for by the annealing technique.

An example shows how the methodology could be implemented in practice. The results are encouraging even though the example may not fully reflect the heterogeneity encountered in practice.

The annealing methodology presented to integrate well test data is quite general. The method has the potential to integrate many disparate data, as long as these data can be quantified to enter a global objective function. For example, multiple-point statistics could be used to input complex curvilinear geological structures and seismic data could be incorporated by adding another component to the global objective function (Deutsch, 1992; Doyen et al., 1989). Other sources of data that could be incorporated are the results of multiple-rate and tracer tests.

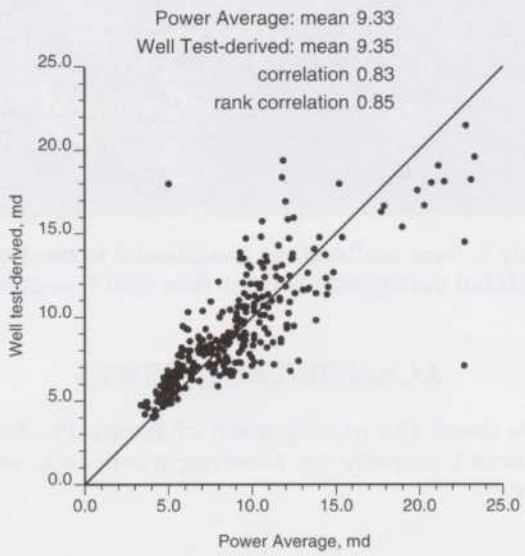

Figure 8. The well test–derived effective permeability versus the power average approximation for the 500 (5 wells × 100 realizations) well tests.

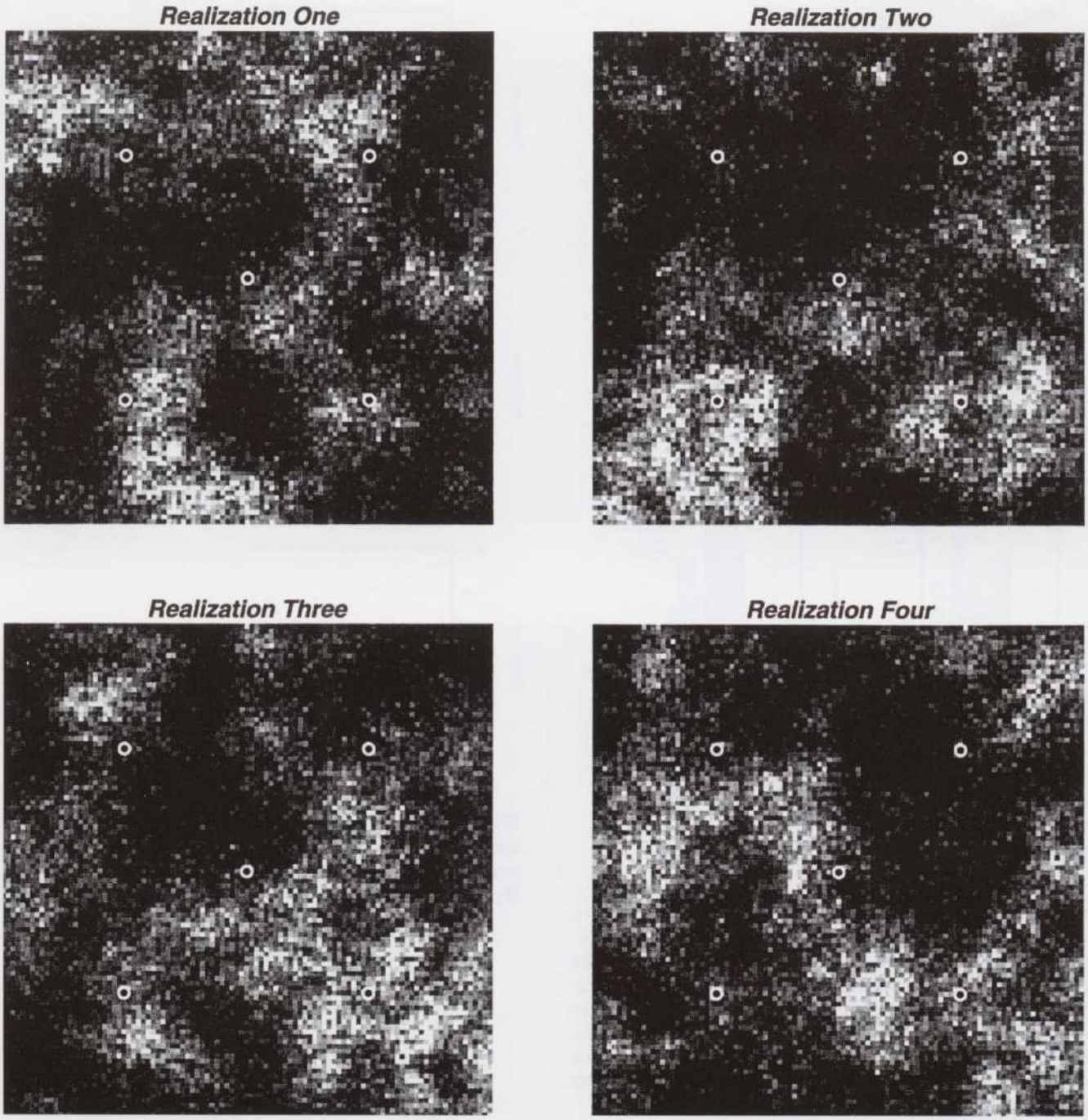

Figure 9. Four realizations conditional to the five data (represented by the black dots), the global histogram, the global variogram, and the five well test–conditioned results.

ACKNOWLEDGMENTS

We thank the management of Exxon Production Research Company for allowing publication of this paper.

REFERENCES

Aarts, E., and J. Korst, 1989, Simulated annealing and Boltzmann machines: New York, John Wiley.

Alabert, F., 1989, Constraining description of randomly heterogeneous reservoirs to pressure test data: a Monte Carlo study: SPE Paper 19600, SPE Annual Conference and Exhibition, Proceedings.

Deutsch, C., 1989, Calculating effective absolute permeability in sandstone/shale sequences: SPE Formation Evaluation, p. 343–348.

Deutsch, C., 1992, Annealing techniques applied to reservoir modeling and the integration of geological and engineering (well test) data: Ph.D. thesis, Stanford University, Stanford, California.

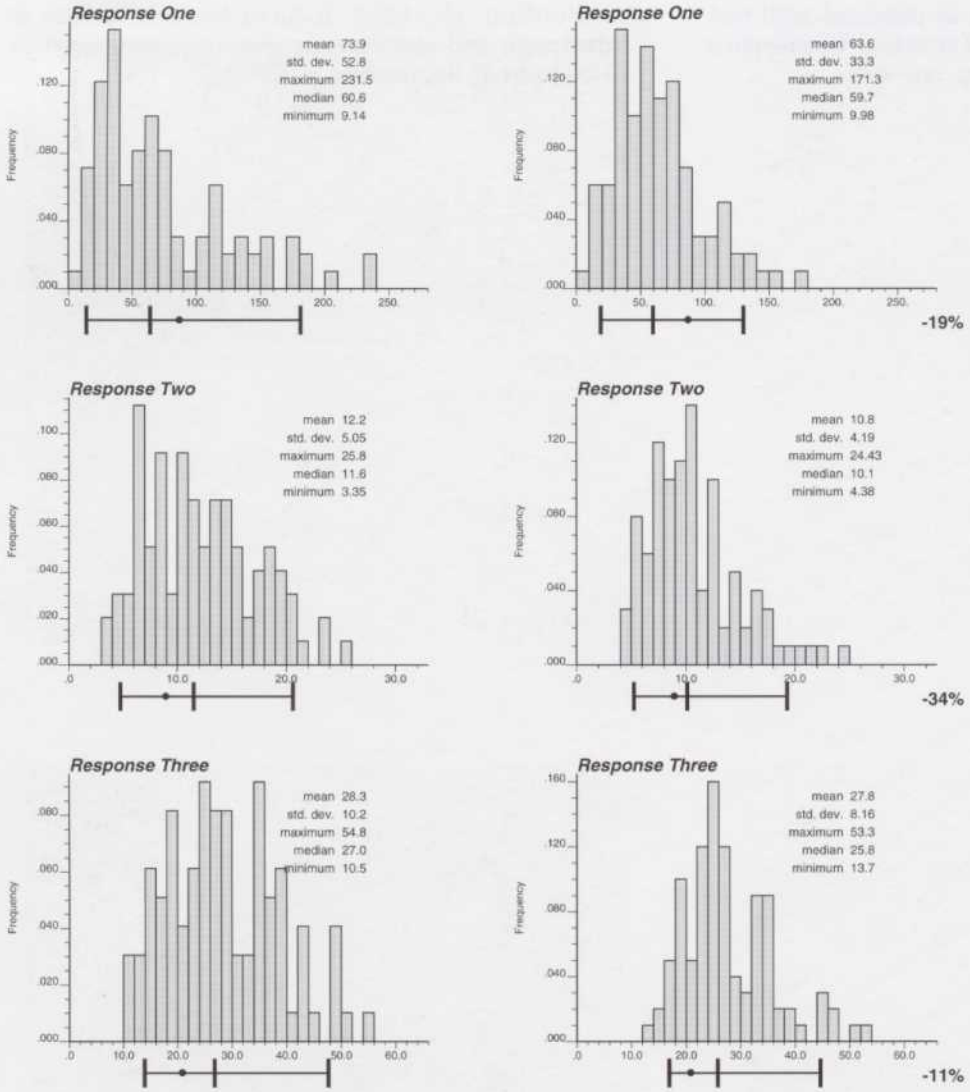

Figure 10. The histograms of the breakthrough time and the final oil in place obtained by running flow simulations on the realizations before (left) and after (right) integrating the well test data. Below the horizontal axis, the black dot is the reference value, the thicker vertical line is the median, and the outermost vertical line represents the 95% probability interval.

Deutsch, C., and A. Journel, 1992, GLSLIB geostatistical software library and user's guide: New York, Oxford University Press.

Doyen, P., 1988, Porosity from seismic data: a geostatistical approach: Geophysics, v. 53, n. 10, p. 1263–1275.

Doyen, P., T. Guidish, and M. de Buyl, 1989, Seismic discrimination of lithology in sand/shale reservoirs: a Bayesian approach: SEG 59th Annual Meeting Extended Abstracts.

Exploration Consultants Limited, 1984, ECLIPSE reference manual: Henley-on-Thames, England, Exploration Consultants Limited.

Haldorsen, H., and E. Damsleth, 1990, Stochastic modeling: Journal of Petroleum Technology, April, p. 404–412.

Hewett, T., 1986, Fractal distributions of reservoir heterogeneity and their influence on fluid transport: SPE Paper 15386.

Horne, R., 1990, Modern well test analysis: Palo Alto, California, Petroway, Inc.

Johnson, P., 1988, The relationship between radius of drainage and cumulative production: SPE Formation Evaluation, March, p. 267–270.

Journel, A., and F. Alabert, 1990, New method for reservoir mapping: Journal of Petroleum Technology, February, p. 212–218.

Journel, A., and C. J. Huijbregts, 1978, Mining geostatistics: New York, Academic Press.

Kirkpatrick, S., C. Gelatt, Jr., and M. Vecchi, 1983, Optimization by simulated annealing: Science, v. 220, n. 4598, p. 671–680.

Korvin, G., 1981, Axiomatic characterization of the general mixture rule: Geoexploration, v. 19, p. 267–276.

Marechal, A., 1984, Kriging seismic data in presence of faults, *in* G. Verly et al., eds., Geostatistics for natural resources characterization: Dordrecht, D. Reidel.

Matheron, G., H. Beucher, H. de Fouquet, A. Galli, D. Guerillot, and C. Ravenne, 1987, Conditional simulation of the geometry of fluvio-deltaic reservoirs: SPE Paper 16753.

Press, W., B. Flannery, S. Teukolsky, and W. Vetterling, 1986, Numerical recipes: New York, Cambridge University Press.

Ramey, H., Jr., 1990, Advances in practical well test analysis: SPE 65th Annual Technical Conference and Exhibition, Proceedings, p. 665–676.

van Poollen, H., 1964, A hard look at radius of drainage and stabilization-time equations: Oil & Gas Journal, September, p. 139–147.